

# Piezoelectricity of Cholesteric Elastomers. 1. Influence of the Helicoidal Pitch on the Piezoelectric Coefficient

Wolfgang Meier and Heino Finkelmann\*

*Institut für Makromolekulare Chemie, Universität Freiburg, Stefan-Meier-Strasse 31, D-7800 Freiburg i. Brsg., FRG*

*Received March 30, 1992; Revised Manuscript Received July 8, 1992*

**ABSTRACT:** Mechanical, optical, and electromechanical investigations were performed on a series of induced cholesteric elastomers. These elastomers are swollen with a chiral low molar mass liquid crystal and exhibit a mechanical coupling coefficient  $U$  that is of the same order of magnitude as that for nonswollen nematic elastomers. Above a certain threshold deformation, a macroscopically uniform orientation of the mesogenic side groups is achieved, with the helicoidal axis oriented parallel to the compression axis. Above this threshold deformation, the helicoidal pitch affinely deforms with elastomer compression. This deformation of the helicoidal superstructure is a basic requirement for piezoelectricity in cholesteric elastomers. Above a threshold deformation electromechanical investigations find a linear relation between voltage and deformation. While the direction of polarization of the elastomer with respect to the helicoidal axis is affected by the surface geometry, the absolute value of the effect remains unchanged. Under a given sample geometry a change of the handedness of the cholesteric helix and investigations with the corresponding nonchiral system prove that only piezoelectricity occurs. Other electromechanical effects like flexoelectricity or electrostriction are negligible. Temperature-dependent measurements find a linear relation between the piezoelectric coefficient and the cholesteric order parameter. Furthermore, the piezoelectric coefficient scales with the reciprocal pitch of the cholesteric elastomers.

## 1. Introduction

In 1880 Curie<sup>1</sup> discovered that a mechanical deformation of certain crystals causes an electric charge at the surface of these crystals. This effect, called piezoelectricity, is characterized by a linear relation between deformation and electric voltage. Today many applications such as sensors, mechanoelectric or acoustoelectric transducers are known for piezoelectric materials.

Piezoelectricity can only be observed in materials having a noncentrosymmetrical structure and elastic properties. Both properties can be found in crystalline materials, the most famous being quartz.

Previous investigations on cholesteric elastomers indicated that uniaxial compression parallel to the helicoidal axis of the cholesteric structure leads to a compression of the helix. Simultaneously an electric charge at the surface of the elastomer is observed. Actually, there exists a linear relationship between deformation of the sample and the electric voltage that resembles piezoelectricity.<sup>3,4</sup> Due to the symmetry of the cholesteric phase, however, this effect is not expected under uniaxial compression. The helicoidal axis and the local nematic director are nonpolar, yielding twofold symmetry axes normal to the helicoidal axis. Under these symmetry conditions piezoelectricity is only expected for shear deformations but not uniaxial deformation parallel to the helicoidal axis.

In contrast to this, Brand proposed a theory for cholesteric elastomers where the helicoidal axis of a cholesteric elastomer is described by a vector.<sup>2</sup> As a consequence the helix axis is polar and uniaxial compression of the helicoidal structure leads to piezoelectricity. The polar axis might be caused by a deviation of the local nematic director from a direction normal to the helicoidal axis or even for a biaxial orientation of the mesogenic units.

The question arises whether the electromechanical effect previously observed actually is caused by piezoelectricity or other effects like flexoelectricity or electrostriction.<sup>2</sup> Furthermore, it has to be analyzed whether shear effects are involved and which molecular properties of the network and the liquid crystalline side chains influence the magnitude of the observed voltage.

Flexoelectricity is defined as the appearance of an induced electric polarization caused by a spatial deformation (e.g., curvature) of the director field of a liquid crystal. Like piezoelectricity, this effect is linear in electric field but arises whether a phase possesses a mirror plane or not. In the case of cholesteric phases, a change in handedness of the helicoidal structure does not affect the sign of flexoelectricity.<sup>5</sup> Electrostriction is an electromechanical effect that always arises when applying mechanical stress to a solid body. Since electrostriction is quadratic in electric field, it is expected to be a higher correction compared to piezoelectricity,<sup>5</sup> which is linear in electric field.

For cholesteric systems piezoelectricity can be easily differentiated from flexoelectricity and electrostriction simply by changing the handedness of the helicoidal structure. Only for piezoelectricity does this cause a change of the sign of the polarization.

Because our previous experiments<sup>4</sup> seem to be consistent with the model of Brand and a polar helicoidal axis, we will briefly outline some of the basic equations describing the piezoelectric effect. On the basis of this model we will analyze whether the electromechanical experiments actually reflect these theoretical statements. To get an idea of the variables that contribute to piezoelectricity, one studies the free energy of such an elastomer. According to the theory of Brand, 1 gives the expansion of the free energy of a cholesteric elastomer. Only terms dealing with deformations and electric field effects are written down explicitly; all other contributions are summarized in  $F_0$ :

$$F = F_0 + \frac{1}{2}Ce^2 + \epsilon^a E^2 + q_0 \zeta^p E e \quad (1)$$

In eq 1  $C$  is Young's modulus,  $e$  the deformation,  $\epsilon^a$  the dielectric permittivity,  $E$  the electric field,  $q_0 = 2\pi/p$  the cholesteric reciprocal pitch, and  $\zeta^p$  the coupling coefficient between  $E$  and  $e$ . Minimizing the free energy with respect to the electric field yields a relation between deformation and the electric field:

$$dF/dE = 2\epsilon^a E + q_0 \zeta^p e = 0 \quad (2)$$

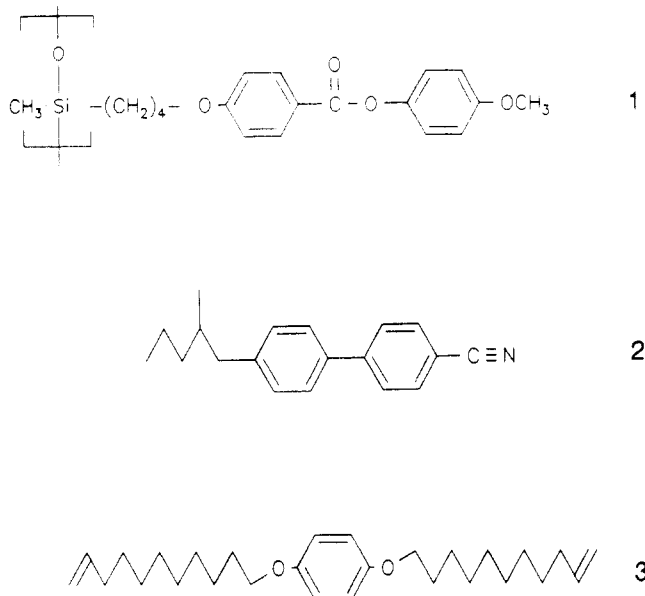


Figure 1. Nematic polymer 1, chiral dopant 2, and cross-linker 3.

or

$$E = -(q_0 \delta^p / 2\epsilon^a) e \quad (3)$$

where the term  $q_0 \delta^p / 2\epsilon^a$  in eq 3 defines the piezoelectric coefficient  $h$ . Here it has to be noted that  $h$  is inversely related to the pitch of cholesteric elastomers. This  $q_0$ -dependence does not occur for other electromechanical effects (flexoelectricity, electrostriction). Consequently, by systematically varying the pitch of cholesteric elastomers, the piezoelectric effect can be easily separated.

In this paper we will describe uniaxial compression experiments on cylindrical cholesteric elastomers in the frame of the theoretical considerations mentioned above. To identify the piezoelectric effect, the cholesteric pitch,  $p$ , of the elastomers is systematically varied. To assure that the variation of the pitch is not coupled to a variation of the dielectric permittivity or the composition of the system, induced cholesteric elastomers are chosen. The variation of pitch is realized by a variation of the enantiomeric excess of the chiral compound inducing the cholesteric phase.

## 2. Experimental Section

**Material.** For measurements of piezoelectric coefficients by compression of a cholesteric elastomer, the helicoidal axis has to be parallel or the local nematic director perpendicular to the compression axis. On the basis of previous results,<sup>4</sup> this orientation behavior is given by the nematic system 1, shown in Figure 1. The cholesteric phase is induced according to well-known procedures by the chiral low molar mass 2'-(2-methylbutyl)biphenyl-4-carbonitrile 2. (R)-, (S)-, and (R/S)-2 were synthesized starting from the corresponding 2-methylbutanol.<sup>6,7</sup> (R)-2-Methylbutanol with an enantiomeric excess of  $ee = 18.9\%$ , necessary for synthesis of (R)-2 was obtained from racemic 2-methylbutanol.<sup>8</sup>

Two polymeric systems have been synthesized: (i) linear reference polymers without cross-linking agent 3 and (ii) cholesteric elastomers with a constant cross-linking density due to a constant mole fraction of 3.

The linear reference polymer is synthesized according to well-known procedures.<sup>9</sup> The average degree of polymerization is  $\bar{P}_n = 100$ . With this linear polymer, the miscibility behavior with 2 and the properties of the induced cholesteric phase are analyzed. These properties can be directly related to the corresponding elastomers as exemplified for the optical properties. In Figure 2 the phase behavior of the binary system 1 and 2 is shown. The

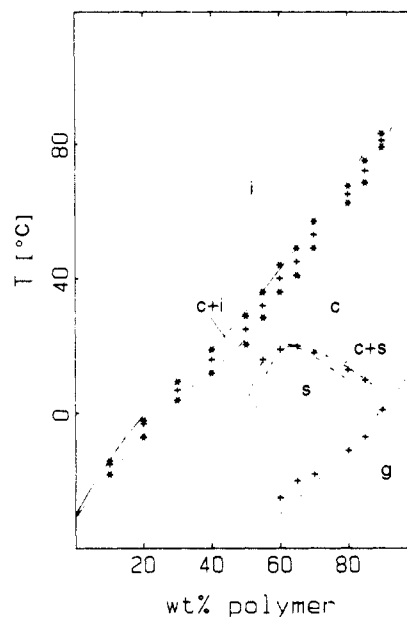


Figure 2. Phase diagram for mixtures of 1 and 2; (+) measured by DSC, (\*) determined by polarizing microscopy (c, cholesteric; i, isotropic; s, smectic; g, glassy).

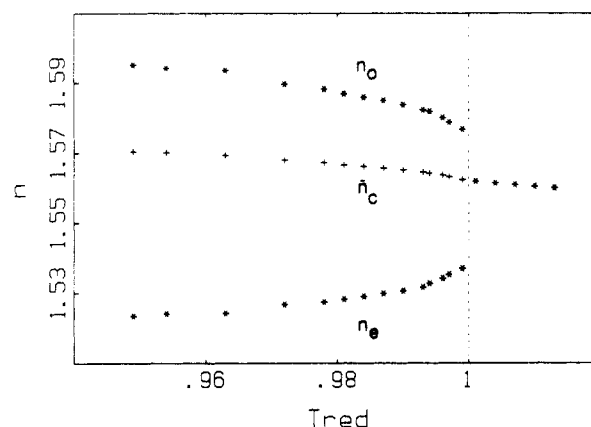
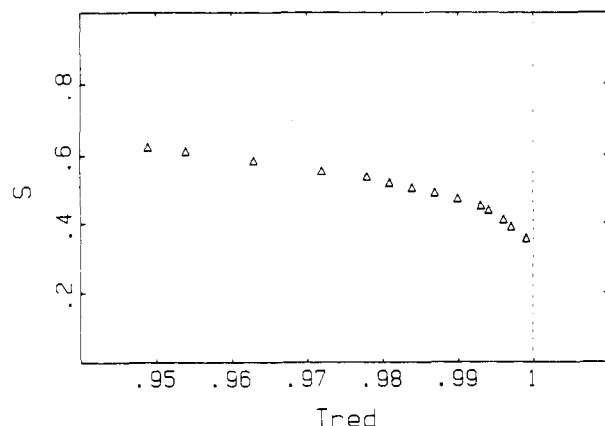


Figure 3. Refraction indices of a mixture of 1 and 2 containing 20 wt % 2 ( $n_e$ , extraordinary refraction index;  $n_o$ , ordinary refraction index;  $\bar{n}_c = 1/3(n_e^2 + 2n_o^2)$ ).

phase diagram exhibits a broad cholesteric phase over the whole concentration range. The cholesteric phase is identified by the Grandjean texture in the polarizing microscope. At low temperatures in the region of 60–80 wt % polymer, an induced smectic phase exists. No crystalline phases could be detected in these mixtures. According to this phase diagram the glass transition temperature of the pure polymer is strongly reduced by 2. A composition which is ideal for the preparation of elastomers is a mixture containing 80 wt % 1 and 20 wt % 2 because it exhibits a broad cholesteric regime (up to 335 K) and a low-temperature glass transition at  $T_g = 255$  K. This mixture is chosen for the synthesis of the elastomers, the characterization of the state of order, and the cholesteric pitch as a function of the optical activity of 2. The state of order is evaluated from birefringence measurements according to the method of Haller.<sup>10,11</sup> In Figure 3 the refractive indices are shown as a function of the reduced temperature. The refractive indices are related to the molecular polarizability  $\alpha$  via the Lorenz-Lorentz equation. Then, the order parameter  $S$  is given by

$$S = [(n_e^2 - n_o^2) / (\bar{n}_c^2 - 1)] / A \quad (4)$$

with  $A = \Delta\alpha / \bar{\alpha}$ ,  $\bar{\alpha} = 1/3(\alpha_e + 2\alpha_o)$  and  $\bar{n}_c^2 = (n_e^2 + 2n_o^2)/3$ .  $n_e$  and  $n_o$  are the extraordinary and the ordinary refraction indices and  $\alpha_e$  and  $\alpha_o$  the corresponding molecular polarizabilities.  $A$  can be determined from the plot of  $\log(S\Delta\alpha/\alpha) = \log[(n_e^2 - n_o^2) / (\bar{n}_c^2 - 1)]$  versus  $-\log[1 - T_{red}]$  by extrapolation to  $T = 0$  K ( $S = 1$ ). If  $A$  is known,  $S$  can be calculated from  $n_e$  and  $n_o$ . In Figure



**Figure 4.** Order parameter  $S$  of the mixture of 1 and 2 containing 20 wt % 2 versus reduced temperature  $T_{\text{red}} = T/T_c$  ( $T$ , measuring temperature;  $T_c$ , cholesteric-to-isotropic phase transformation temperature).

4 the order parameter  $S$  as a function of temperature is shown. The results are in good agreement with previous results.<sup>12</sup>

The cholesteric pitch is determined by selective reflection of circularly polarized light that arises from the helicoidal superstructure. The wavelength of selective reflection,  $\lambda_R$ , is directly connected to the pitch  $p$  of the cholesteric helix by the relation  $\lambda_R = \bar{n}p$ , where  $\bar{n}$  is the average refraction index of a corresponding nematic layer, that can be calculated from the data of Figure 3.<sup>13,14</sup> To determine variation of  $p$  with a change in the enantiomeric excess of 2,  $\lambda_R$  is measured as a function of the enantiomeric excess. The enantiomeric purity of 2 is systematically varied by substitution of chiral 2 with racemic 2. This procedure guarantees that  $\bar{n}$  remains constant for all mixtures and, consequently,  $\lambda_R$  is always directly proportional to  $p$ . For  $\lambda_R < 2000$  nm the wavelength of selective reflection is determined by circular dichroism measurements using a UV-vis photospectrometer and for  $\lambda_R > 2000$  nm using the optical rotation dispersion (ORD) following the formalism of de Vries.<sup>14</sup> The ORD measurements find that (*S*)-2 induces a right-handed and (*R*)-2 a left-handed helix. The temperature dependence of  $\lambda_R$  can be neglected in the temperature range between isotropic-to-cholesteric phase transformation temperature and 30 °C. As known from low-molar-mass cholesteric phases a linear relation exists between  $1/p$  and the enantiomeric excess (ee) of 2. For the racemic 2 the system is nematic ( $1/p = 0$ ).

The corresponding elastomers are synthesized in a two-step process in the isotropic state. According to previous, detailed measurements on nematic elastomers, the network formation in the isotropic state is necessary to avoid induced network anisotropy.<sup>15</sup> In the first step a linear polymer is prepared which still contains 4 mol % reactive Si-H monomer units. This polymer is mixed with an adequate quantity of 2 and the bifunctional cross-linking agent 3. Within 4 h at a temperature of 353 K (in the isotropic state) the cross-linking reaction is completed. The resulting elastomers are cylindrical in shape with a height of  $6.0 \pm 0.1$  mm and a diameter of  $14.0 \pm 0.1$  mm. The cholesteric-to-isotropic phase transformation temperature was determined to be  $T_c = 338 \pm 0.5$  K (DSC) and  $T_g = 253$  K for the whole series of elastomers. For two samples the wavelength of selective reflection,  $\lambda_R$ , is measured by circular dichroism. The optical rotation ( $p > 2000$  nm) measurements fail due to the large values of the optical rotation of the cylindrical elastomers. These elastomers exhibit the same values in  $\lambda_R$  as the corresponding linear polymer systems with an accuracy of  $\pm 5$  nm (see Table I). Therefore, the values of the linear polymer are taken to be valid also for the corresponding elastomers.

**Measurements.** Optical measurements of the elastomers are performed on a UV-vis photospectrometer (330 photospectrometer, Perkin-Elmer).  $\lambda_R$  as a function of deformation is determined in a temperature-controlled chamber. Elastomers are compressed with an accuracy of  $\pm 10$   $\mu\text{m}$ . Temperature is regulated to a constant value within  $\pm 0.1$  K.

Mechanical and electromechanical measurements are performed in a self-constructed, computer-controlled apparatus. The

**Table I**  
Enantiomeric Excess (ee) and the Wavelength of Selective Reflection ( $\lambda_R$ ) for the Elastomers and Corresponding Linear Polymer Systems

elastomer	ee of 2 (%)	$\lambda_R$ (nm)	
		elastomer	polymer
E100	100	1286	1290
E75	75	1708	1710
E50	50		2560
E19	19		6910
E0	0		
E-19	-19		6780

sample is compressed to an accuracy of  $\pm 1.5$   $\mu\text{m}$  by two simultaneously working displacement disks. Stress is measured by a force transducer as a function of the deformation. Simultaneously electric voltage is measured with a Keithley electrometer voltmeter (input resistance  $> 5 \times 10^{13}$   $\Omega$ ) having an analogue output to the computer. The sample is fixed in a closed heating chamber. Temperature is regulated to a constant value with an accuracy of  $\pm 0.04$  K all along the sample. The experiments were carried out statically according to the following procedure: the unloaded sample is compressed and the voltage is analyzed until a maximum value is observed. Thereafter the elastomer is released for the next measuring cycle. Because the diameter of the electrodes is larger than the diameter of the elastomers, the measured voltage has to be corrected by a factor

$$C = \{A_s + (\epsilon_{el} - 1)A_{el}\} / (\epsilon_{el}A_{el}) \quad (5)$$

where  $A_s$  is the area of the electrodes,  $\epsilon_{el}$  is the dielectric permittivity of the elastomers, and  $A_{el}$  is the area of the cylindrical elastomer in contact with the electrodes. With the dimensions of the setup and  $\epsilon_{el}^{16} \approx 7.5$ , the factor  $C \approx 1.2$ . Since  $C$  is the same for all elastomers ( $\epsilon_{el} = \text{constant}$ ) and only relative values are of interest, in the following, the noncorrected voltages are discussed.

### 3. Results and Discussion

**Mechanical Investigations.** To get detailed information about the stress-induced orientation process from the nonordered (polydomain) to the macroscopically uniformly ordered state (monodomain), mechanical properties of the elastomers are investigated. As the mechanical behavior of the different samples is the same within experimental error in Figure 5 the nominal stress  $\sigma_n$  is shown as a function of deformation  $\lambda$  only for elastomer E100 at different temperatures. Similar to previous results<sup>4</sup> in the cholesteric phase the nominal stress remains nearly constant at  $\sigma_n \approx 0$  N mm<sup>-2</sup> for a broad deformation regime. In this region a polydomain/monodomain transition occurs, which is correlated to a considerable change in the sample dimensions<sup>4</sup>. Above this region, a monodomain exists with linear stress-strain behavior. The linear extrapolation of the stress-strain curve to  $\sigma_n = 0$  leads to a threshold deformation  $\lambda_m$ , that defines the deformation of the elastomer necessary to obtain the macroscopically aligned system with length  $L_{\text{mon}}$ . The inverse of  $L_{\text{mon}}$  characterizing the macroscopic anisotropy of the elastomer, as a function of temperature, is shown in Figure 6. Interestingly, the slope of  $1/L_{\text{mon}}(T)$  resembles the slope of the order parameter of the elastomers  $S(T)$  shown in Figure 4. Actually, a correlation between  $1/L_{\text{mon}}$  and  $S$  exhibits a linear behavior in analogy to stress-strain measurements on nematic elastomers<sup>17,18</sup> which is shown in Figure 7. For simplification in Figure 7, the length of the monodomain  $L_{\text{mon}}$  is related to the length of the monodomain  $L_{\text{mon},T_c}$  at the cholesteric-to-isotropic transformation temperature  $T_c$ . These measurements directly prove the linear relationship between the state of order and the macroscopically anisotropic dimensions of the network. From Figure 7 we can obtain another parameter, the coupling coefficient  $U$  of the elastomer, that is

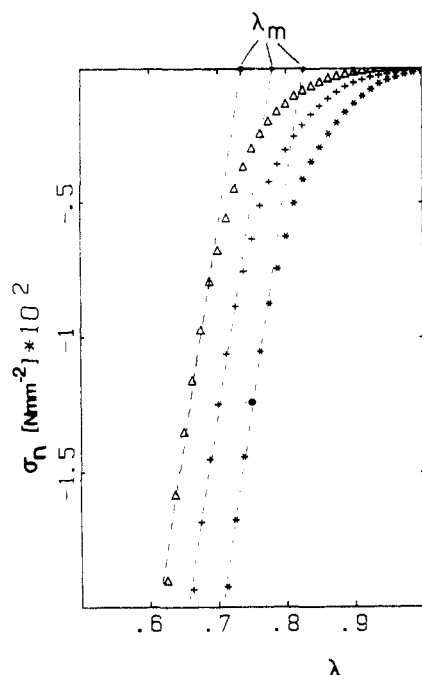


**Figure 5.** Nominal stress  $\sigma_n$  versus deformation  $\lambda$  of elastomer E100 for several reduced temperatures  $T_{red}$ : ( $\Delta$ )  $T_{red} = 0.956$ ; (+)  $T_{red} = 0.970$ ; (\*)  $T_{red} = 0.985$ . The extrapolated deformation  $\lambda_m$  indicates the threshold deformation necessary to obtain the macroscopically ordered elastomer.

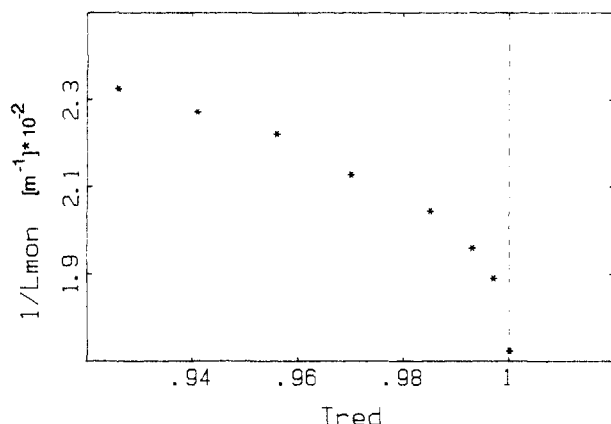


**Figure 6.** Reciprocal length  $1/L_{mon}$  of the macroscopically uniform oriented elastomer versus reduced temperature  $T_{red}$ .

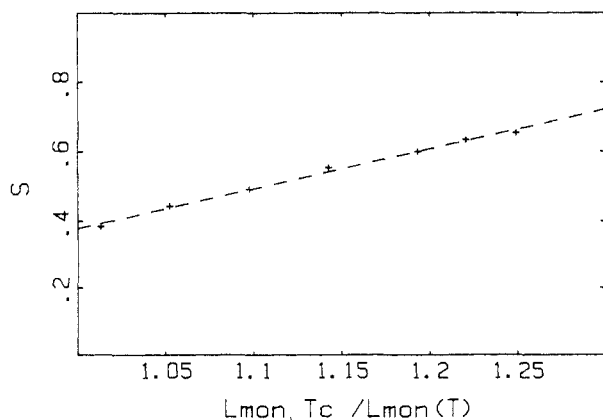


**Figure 7.** Order parameter  $S$  as a function of the reduced reciprocal length of the macroscopically uniform oriented elastomer  $L_{mon, T_c}/L_{mon}(T)$  ( $L_{mon, T_c}$ , length of the macroscopically ordered elastomer at  $T_c$ ).

important for later discussions. The coupling coefficient  $U$  characterizes the effect of the mechanical field on the state of order of the elastomers, which can be described

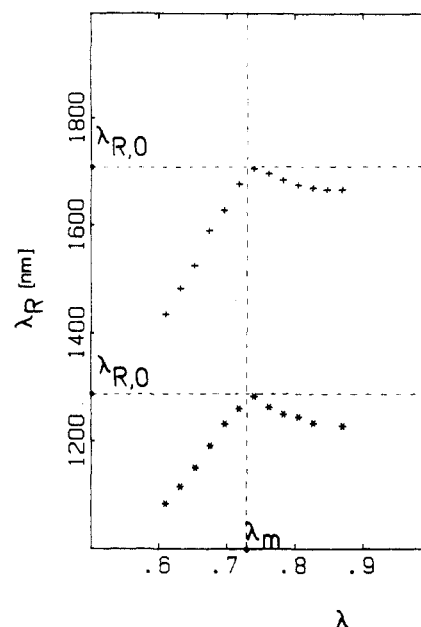


**Figure 8.** Wavelength of selective reflection  $\lambda_R$  for elastomer E100 (\*) and elastomer E75 (+) at  $T_{red} = 0.956$  versus deformation  $\lambda$  of the sample.  $\lambda_{R,0}$  indicates  $\lambda_R$  of the noncompressed helicoidal structure.

by

$$S = -\sigma/U + (\mu/U)\lambda \quad (6)$$

where  $\mu$  is the modulus and  $\lambda$  the deformation of the macroscopically ordered elastomer. With eq 6, we find  $U = (1.3 \pm 0.5) \times 10^4 \text{ J m}^{-3}$  which is in good agreement with the results for nematic elastomers.<sup>17,18</sup>

**Mechano-optical Investigations.** Previous investigations showed that uniaxial compression of the elastomers occurs parallel to the helicoidal axis. According to Brand,<sup>2</sup> under these conditions the helicoidal structure should be compressed and piezoelectricity should be observed. To quantify the stress-pitch relation for elastomers E100 and E75, optomechanical measurements are performed. The wavelength of selective reflection,  $\lambda_R$ , is measured as a function of compression. Figure 8 shows the experimental results that can also be directly related to the stress-strain measurements above. In the compression range, where elastomers exhibit a polydomain structure, a slight change of  $\lambda_R$  occurs with compression due to the formation of the macroscopically uniformly oriented sample. Below  $\lambda_m$  a linear relation between  $\lambda_R$  and  $\lambda$  exists consistent with the mechanical measurements. To clarify whether the helix deformation occurs affinely with the network deformation in Figure 9, the relative change of the reflection wavelength  $\lambda_{helix} = \lambda_R/\lambda_{R,0} = p/p_0$  ( $\lambda_{R,0}$ , wavelength of the selective reflection of the undeformed helix with pitch  $p_0$ ) is shown as function of the relative deformation  $\lambda_{mon} = L/L_{mon}$  of the macroscopically ordered network. Interestingly, for both elastomers the slope is  $0.9 \pm 0.15$ . This result indicates that the deformation of the cholesteric helix seems to follow affinely the deformation of the network. It should be noted that the affine deformation of the helix resembles the deformation of the helicoidal structure of low-molar-mass liquid crystals by the Cano wedge method.<sup>19,20</sup> Here the pitch of the cholesteric phase follows affinely the variation of a layer thickness, due to fixed boundary conditions.

**Electromechanical Investigations.** Mechanical and optical investigations reveal that a macroscopically uniform oriented cholesteric elastomer is obtained below  $\lambda_m$ , where the helicoidal axis is parallel to the axis of

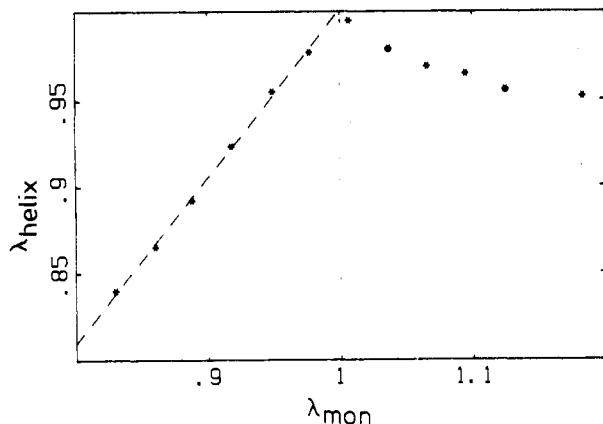


**Figure 9.** Deformation of the helicoidal structure  $\lambda_{\text{helix}} = p/p_0$  versus deformation of the macroscopically uniformly oriented elastomer sample  $\lambda_{\text{mon}} = L/L_{\text{mon}}$  at  $T_{\text{red}} = 0.956$ .

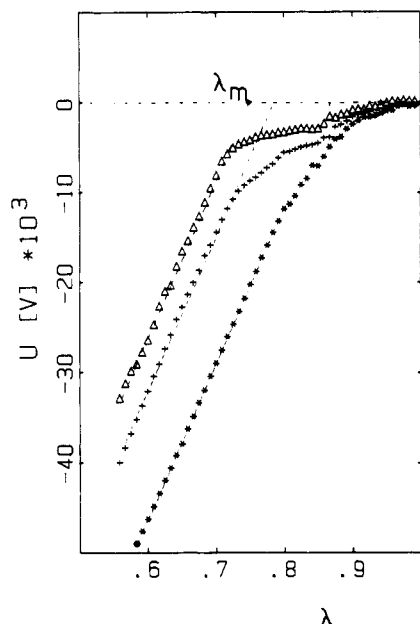


**Figure 10.** Piezoelectric voltage  $U$  versus deformation  $\lambda$  of elastomer E100 for different reduced temperatures  $T_{\text{red}}$ : ( $\Delta$ )  $T_{\text{red}} = 0.956$ ; (+)  $T_{\text{red}} = 0.970$ ; (\*)  $T_{\text{red}} = 0.985$ .

compression. Further deformation yields a significant decrease in pitch. Figure 10 shows the electric voltage  $U$  as a function of sample deformation for three selected temperatures. Actually, when the macroscopically uniform oriented system is obtained below  $\lambda_m$ , a linear relation is found between  $U$  and  $\lambda$ , as expected for piezoelectricity. Extrapolation of the linear part of the  $U(\lambda)$  curve to  $U = 0$  leads to a threshold deformation that coincides well with the results of the mechanical and optical investigations. The slope of  $U(\lambda)$  gives directly the piezoelectric coefficient of the macroscopically uniformly ordered cholesteric elastomer.

It should be noted that the sign of the voltage and the piezoelectric coefficient have to be related to a polar axis, which should not exist in cylindrical samples. However, as mentioned in the Experimental Section, the samples slightly deviate from cylindrical symmetry. Due to the preparation process an "upper surface" can be identified having not a planar but a slightly concave shape. Actually, the sign of the voltage can always be related to this surface. When the sample is turned upside down, the voltage changes sign at the measuring cell, but the absolute value of the slope of the  $U(\lambda)$  curve remains unchanged. To identify whether this concave surface geometry determined

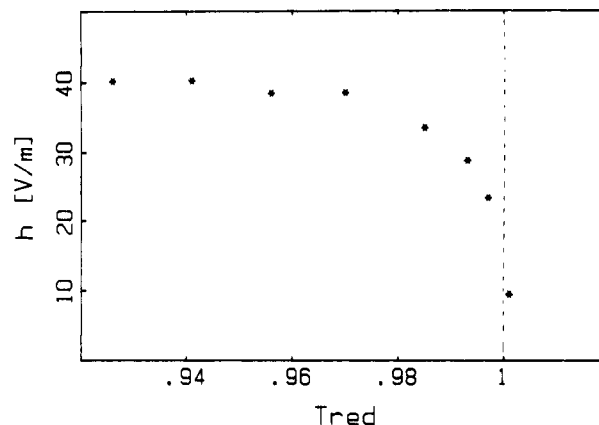


**Figure 11.** Piezoelectric coefficient  $h$  versus reduced temperature  $T_{\text{red}}$  for elastomer E100.

the sign of the electromechanical effect, samples were prepared with modified surfaces. Actually, for convex surfaces with a different curvature the effect changes sign, but within experimental error the slope of the  $U(\lambda)$  curve is not affected. Obviously, this surface geometry induces the direction of the polarization due to the gradient in the mechanical field. Additional measurements have to be performed to quantify and clarify this effect.

In Figure 11 the piezoelectric coefficient  $h$  is shown versus reduced temperature for elastomer E100. Similar to the reciprocal length of the uniformly aligned sample, the temperature dependence resembles the temperature dependence of the order parameter  $S$  in Figure 4. According to eq 3  $h$  scales with  $\zeta^p/\epsilon^a$  and  $\epsilon^a$  scales with  $S$ . Therefore, we can relate the inverse order parameter  $1/S$  to the piezoelectric coefficient  $h$ . Actually, a linear relation is obtained (Figure 12a). However, as shown in Figure 12b, a correlation of  $S$  to  $h$  also fits a linear relation well. This result is consistent with  $\zeta^p$  scaling with  $S^2$  and  $\epsilon^a$  with  $S$  as mentioned above. As  $\zeta^p$  is a kind of elastic constant, this is not too unreasonable as we know, e.g., that the Frank constants scale with  $S^2$ . Whether  $h$  scales with  $1/S$  or with  $S$  cannot be decided from Figure 12a,b and has to be clarified by further investigations. The correlation between the piezoelectric coefficient and the order parameter reflects a coupling and shows that the piezoelectric effect of cholesteric elastomers directly depends on the state of order of the liquid crystalline phase structure. It should be noted that this correlation does not exist in conventional piezoelectrics and has to be considered in a theoretical description of this effect.

According to eq 3 the piezoelectric coefficient is directly proportional to the reciprocal pitch of the cholesteric phase. To prove this relation, the enantiomeric excess of the elastomers is varied according to Table I, which only affects the pitch but not the composition nor the dielectric properties of the elastomers. For these different elastomers, the voltage  $U$  is shown as a function of the deformation  $\lambda$  at  $T_{\text{red}} = 0.985$  in Figure 13. As expected from eq 3 the slope of  $U(\lambda)$  decreases with increasing pitch and becomes zero for the racemic system. When the chirality of 2 changes from  $S$  to  $R$ , the sign of the effect changes according to the change of the handedness of the pitch. We note that for  $p = \infty$  no voltage appears under compression. This result proves that electrostriction and flexoelectricity do not occur. Moreover, electrostriction can be neglected because of the linear behavior of the  $U(\lambda)$  curves below  $\lambda_m$ . The threshold deformation  $\lambda_m$  can be excellently extrapolated from all curves, indicating that the variation of the enantiomeric excess actually does not affect the mechanical properties of the elastomers. Fur-

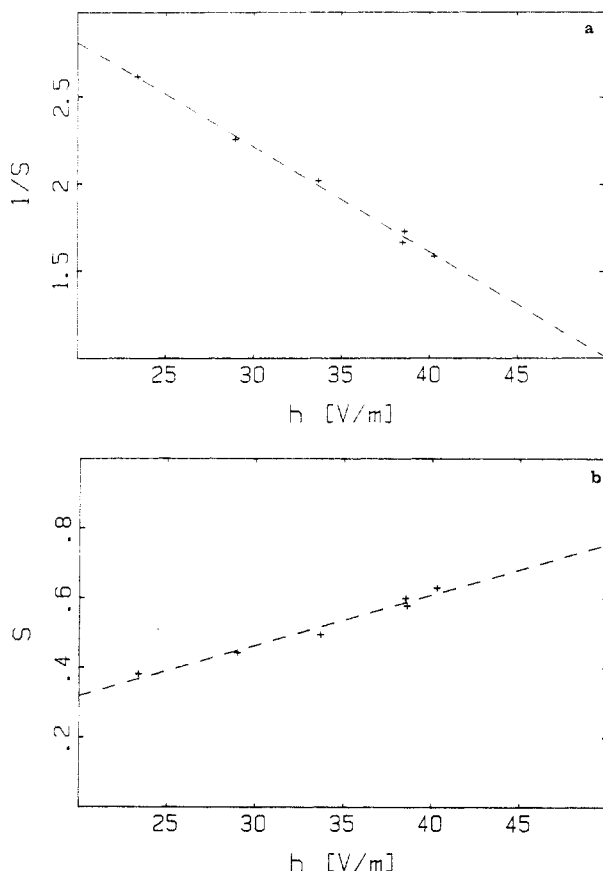


**Figure 12.** (a) Inverse order parameter  $1/S$  of the cholesteric phase versus piezoelectric coefficient  $h$ . (b) Order parameter  $S$  of the cholesteric phase versus piezoelectric coefficient  $h$ .

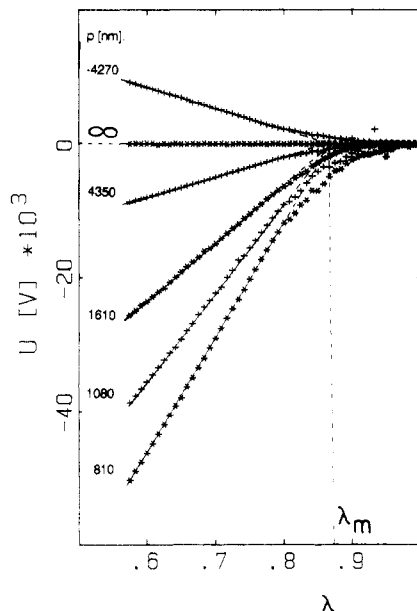


**Figure 13.** Piezoelectric voltage  $U$  versus deformation  $\lambda$  for six samples with different pitch (refer to Table I) of the cholesteric phase at  $T_{\text{red}} = 0.985$ .  $\lambda_m$  indicates the deformation necessary to obtain the macroscopically ordered elastomers.

thermore, this extrapolation to  $\lambda_m$  also proves that the synthesis route yields identical polymer networks. In Figure 14 the piezoelectric coefficients obtained from Figure 13 are plotted versus the reciprocal pitch for the selected reduced temperature  $T_{\text{red}} = 0.970$ . An excellent linear relation exists which proves eq 3 with respect to the pitch dependence of the piezoelectric effect. The slope of this relation reflects the dielectric properties of the system

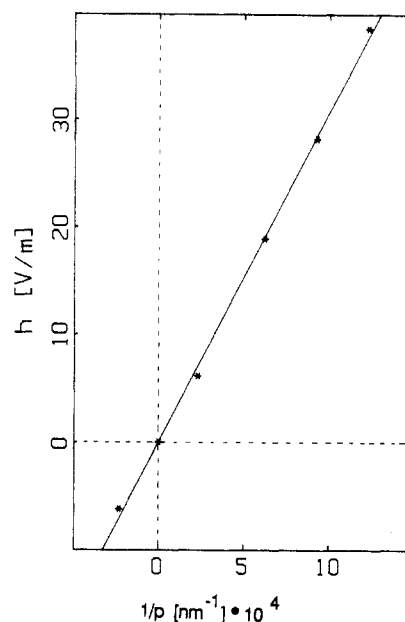


**Figure 14.** Piezoelectric coefficient  $h$  for six different elastomers versus the reciprocal pitch  $1/p$  of the elastomers at  $T_{\text{red}} = 0.970$ .

as well as the coupling coefficient  $\beta$  between electric field and deformation. Further investigations have to clarify the significance of these different terms.

#### 4. Conclusions

Our experiments clearly show that for cholesteric elastomers a linear electromechanical effect exists. This effect is not due to flexoelectricity but is similar to piezoelectricity of solid-state materials. The temperature dependence of the piezoelectric coefficient shows that in cholesteric elastomers an additional coupling between the piezoelectric coefficient and the order parameter of the liquid crystalline phase has to be taken into account. This indicates that piezoelectricity of liquid crystalline elastomers cannot be described in terms of a classical solid body effect. This "nonclassical" behavior is also proved by the fact that the results of direct and converse piezoelectric measurements cannot be correlated if a coupling is neglected.<sup>21</sup> Both a theoretical understanding of the effect and optimization of liquid crystalline elastomer for application make it necessary to get an idea about the influence of the chemical constitution of the mesogenic units on piezoelectricity in cholesteric elastomers. Although our experiments prove the linear relation between the piezoelectric coefficient and the reciprocal pitch, up to now we still do not know in which way a variation of the molecular properties influences the magnitude of the observed effect. In this context it will be of interest to investigate the influence of a variation of the anisotropy of the dielectric permittivity  $\Delta\epsilon$  of the mesogenic units. For our samples the sign of the effect can be attributed to the surface curvature. Here it has to be quantified whether only the resulting mechanical field gradient causes the polar axis or whether the polar axis is actually an intrinsic quantity of these elastomers.

**Acknowledgment.** The authors are indebted to H. Brand for many stimulating discussions and to P. E. Cladis for helpful comments. This research was supported by Deutsche Forschungsgemeinschaft (SFB 60) and the Fonds der Chemischen Industrie. W. M. thanks the Fonds der Chemischen Industrie for the Chemiefonds Stipendium. The authors are also indebted to R. B. Meyer. He pointed

out that according to the established picture of the cholesteric phase no polar axis exists and that under these conditions the effect described in this paper should be due some components of neat shear to the sample. He also pointed out that some gradients in the sample properties may cause the effect and the sign. These arguments have been considered in revising this manuscript.

## References and Notes

- (1) Curie, J.; Curie, P. C. R. *Hebd. Seances Acad. Sci.* **1890**, *91*, 294.
- (2) Brand, H. R. *Makromol. Chem., Rapid Commun.* **1989**, *10*, 441.
- (3) Vallerien, S. U.; Kremer, F.; Fischer, E. Q.; Kapitza, H.; Zentel, R.; Poths, H. *Makromol. Chem., Rapid Commun.* **1990**, *11*, 593.
- (4) Meier, W.; Finkelmann, H. *Makromol. Chem., Rapid Commun.* **1990**, *11*, 599.
- (5) Brand, H. R.; Pleiner, H. *Makromol. Chem., Rapid Commun.* **1990**, *11*, 607.
- (6) Kaszynski, P.; Jawdosnik, M. *Mol. Cryst. Liq. Cryst.* **1989**, *174*, 21.
- (7) Gray, G. W.; McDonnell, D. G. *Mol. Cryst. Liq. Cryst.* **1976**, *37*, 189.
- (8) Barrow, F.; Atkinson, R. G. *J. Chem. Soc.* **1939**, 638.
- (9) Finkelmann, H.; Kock, H. J.; Rehage, G. *Makromol. Chem., Rapid Commun.* **1981**, *2*, 317.
- (10) Haller, I.; Huggins, H. A.; Lilienthal, H. R.; McGuire, T. R. *J. Phys. Chem.* **1973**, *77*, 950.
- (11) Haller, I. *Prog. Solid State Chem.* **1975**, *10*, 103.
- (12) Finkelmann, H.; Benthack, H.; Rehage, G. *J. Chem. Phys.* **1983**, *80* (1), 163.
- (13) Stegemeyer, H. *Ber. Bunsen-ges. Phys. Chem.* **1974**, *78* (9), 860.
- (14) de Vries, H. *Acta Crystallogr.* **1951**, *4*, 219.
- (15) Küpfer, J.; Finkelmann, H. *Makromol. Chem., Rapid Commun.* **1991**, *12*, 717.
- (16) Scheuermann, H., private communication.
- (17) Kaufhold, W.; Finkelmann, H.; Brand, H. R. *Makromol. Chem.* **1991**, *192*, 2555.
- (18) Kaufhold, W. Ph.D. Thesis, Universität Freiburg, Freiburg, FRG, 1991.
- (19) Grandjean, F. C. R. *Hebd. Seances Acad. Sci.* **1921**, *172*, 71.
- (20) Cano, R.; Chatelain, P. R. C. *Hebd. Seances Acad. Sci.* **1971**, *253B*, 1815.
- (21) Hirschmann, H.; Meier, W.; Finkelmann, H., to be published.